3.3. Melanin-Like Pigments Synthesis by Sc-Ms1 Tyrosinase and Tv Laccase

Sc-Ms1 tyrosinase (47.6 U mg^{-1}) and Tv laccase (12.9 U mg^{-1}) in 100 mM phosphate buffer at pH 7 were used to synthesize eumelanin in the presence of excess dopa (6.57 mg/mL) as the substrate [6]. The reactions were followed for 16 h. The formation of an insoluble black pigment was obtained. Cysteinyldopa was synthesized using Tv laccase (12.9 U mg^{-1}) with a dopa:cysteine molar ratio of 1:2. A reddish powder was obtained [6]. Samples were dried under nitrogen flux for approximately 5 h and then analyzed in the powder form.

3.4. UV-Visible and FT-IR Spectroscopies

A qualitative analysis of melanin samples was performed using UV-Vis near infrared (NIR) spectrometer Lambda 900/Perkin Elmer Instruments (Norwalk, CT, USA). The spectra were recorded in the wavelength range of 200 to 800 nm.

Melanin powders were IR characterized using a Nicolet FT-IR iS50 (Thermo Fischer Scientific, Madison, WI, USA). Samples were prepared as powder dispersions in KBr tablets and directly analysed.

3.5. Electron Paramagnetic Resonance Spectroscopy

The melanin powder samples were investigated using cw-multifrequency EPR at S-, X-, and Q-band microwave frequencies at room temperature. Each sample was prepared by transferring the melanin powder in an open EPR suprasil tubes (Cortecnet, Voisins-le-Bretonneux, France). The EPR measurements at different frequencies for each sample were collected using the same tube prepared for the Q-band measurements. All EPR microwave bridges were operating on a E580 ELEXSYS spectrometer (Bruker Biospin GmbH, Rheinstetten, Germany), equipped with the following setup: Bruker SuperQ-FT microwave bridge with *ER 5107D2* probehead for Q-band, Bruker ER 049X microwave bridge with 4122SHQE/0208 cavity for X-band, and a SB-1111 microwave bridge (Jag-Mar, Krakow, Poland) with a Loop Gap Resonator probe (Medical Advances Inc., Milwaukee, WI, USA) for S-band. All EPR spectra were recorded using the following parameters: 20 mT scan width and 0.2 mT modulation amplitude. The modulation frequency was 100 KHz for X- and S-bands and 50 KHz for Q-band measurements. A Strong Pitch standard (g = 2.0028) was used for g-value determination. Graphs were built using EasySpin package (ver. 5.2.16) on MATLAB R2017a. Simulations of the EPR spectra were performed using the routine "pepper" of the EasySpin package [42]. The automated best fittings were obtained using the Nelder-Mead (Simplex) method.

4. Conclusions

Melanins are heterogeneous macromolecules with persistent free radical signals. The EPR is the elective technique used for the characterization of their paramagnetism. A multifrequency EPR approach at S-, X-, and Q-bands was used to identify and characterize the melanin exopigment produced by the *Streptomyces cyaneofuscatus* actinobacteria. This brownish colored pigment revealed an EPR signal typical of melanin polymers. The strategy used here was to calculate the g_{iso} value from the S-band measurements, the linewidths and the coupling constants from the X-band spectra, and the Q-band was used to separate the different contributions based on their anisotropies. In particular, the spectral lineshape recorded at Q-band showed the presence of different contributions. Given the natural water soluble melanin complex architecture, we successfully characterized the complex in terms of eumelanin/pheomelanin enzymic synthesized pigments. The insoluble eumelanin and cysteynildopa pigments were synthesized using Tv laccase in the presence of dopa (eumelanin) and a 1:2 dopa:cysteine molar ratio (cysteinyldopa). Conversely, the Sc-Ms1 tyrosinase in the presence of dopa formed an insoluble pigment composed of an excess of eumelanin and some pheomelanin due to the natural origin of the enzyme. This study can help clarify the composition of different melanins with the valuable assistance of Q-band EPR experiments. Due to their physico-chemical characteristics, melanin pigments can be used in different applications, ranging from UV-Vis protectants, radical scavengers,

conductive materials, electrochemical applications, and in medical applications to understand melanin related diseases. In this context, for a better understanding of the electronic structure of different melanins and their characterization in solid states, microwave power saturation EPR measurements and pulsed Q-band relaxation experiments are being undertaken.

Author Contributions: M.A.K. was the first experimenter, participated in analyzing the data and in the manuscript preparation; M.H. prepared the microorganism cultures in different media and isolated enzymes. J.C. performed the enzymic synthesis and the spectrophotometric measurements. M.C.B. and R.B. participated to the EPR data analysis. L.T., I.S., S.P. and G.M.R. participated in the cultivation and preparation of the biological samples. R.P. conceived and designed the experiments, analyzed all the data and wrote the paper. All authors read and approved the final manuscript.

Funding: This research received no external funding.

Acknowledgments: The authors thank the Algerian Ministry for Higher Education and scientific research for the fellowship to M.H. and A. Magnani and M. Consumi for the assistance and useful discussion with FT-IR experiments. CSGI (Consorzio per lo Sviluppo dei Sistemi a Grande Interfase), Florence, Italy and MIUR for the Dipartimento di Eccellenza 2018-2022 grant are gratefully acknowledged.

Conflicts of Interest: The authors declare no conflict of interest.

References

1. Solano, F. Melanin and melanin-related polymers as materials with biomedical and biotechnological applications—Cuttlefish ink and mussel foot proteins as inspired biomolecules. *Int. J. Mol. Sci.* **2017**, *18*, 1561. [CrossRef] [PubMed]
2. Meredith, P.; Sarna, T. The physical and chemical properties of eumelanin. *Pigment Cell Res.* **2006**, *19*, 572–594. [CrossRef] [PubMed]
3. D'Ischia, M.; Napolitano, A.; Pezzella, A.; Meredith, P.; Sarna, T. Chemical and structural diversity in eumelanins: Unexplored bio-optoelectronic materials. *Angew. Chem. Int. Ed.* **2009**, *48*, 3914–3921. [CrossRef] [PubMed]
4. Felix, C.C.; Hyde, J.S.; Sarna, T.; Sealy, R. Interactions of Melanin with Metal Ions. Electron Spin Resonance Evidence for Chelate Complexes of Metal Ions with Free Radicals. *J. Am. Chem. Soc.* **1978**, *100*, 3922–3926. [CrossRef]
5. Solano, F. Melanins: Skin Pigments and Much More—Types, Structural Models, Biological Functions, and Formation Routes. *New J. Sci.* **2014**, *2014*, 498276. [CrossRef]
6. D'Ischia, M.; Wakamatsu, K.; Napolitano, A.; Briganti, S.; Garcia-Borron, J.C.; Kovacs, D.; Meredith, P.; Pezzella, A.; Picardo, M.; Sarna, T.; et al. Melanins and melanogenesis: Methods, standards, protocols. *Pigment Cell Melanoma Res.* **2013**, *26*, 616–633. [CrossRef] [PubMed]
7. Iacomino, M.; Mancebo-Aracil, J.; Guardingo, M.; Martín, R.; D'Errico, G.; Perfetti, M.; Manini, P.; Crescenzi, O.; Busqué, F.; Napolitano, A.; et al. Replacing nitrogen by sulfur: From structurally disordered eumelanins to regioregular thiomelanin polymers. *Int. J. Mol. Sci.* **2017**, *18*, 2169. [CrossRef] [PubMed]
8. Mostert, A.B.; Hanson, G.R.; Sarna, T.; Gentle, I.R.; Powell, B.J.; Meredith, P. Hydration-controlled X-band EPR spectroscopy: A tool for unravelling the complexities of the solid-state free radical in eumelanin. *J. Phys. Chem. B* **2013**, *117*, 4965–4972. [CrossRef] [PubMed]
9. Chen, C.T.; Chuang, C.; Cao, J.; Ball, V.; Ruch, D.; Buehler, M.J. Excitonic effects from geometric order and disorder explain broadband optical absorption in eumelanin. *Nat. Commun.* **2014**, *5*, 3859. [CrossRef] [PubMed]
10. D'Ischia, M.; Napolitano, A.; Ball, V.; Chen, C.T.; Buehler, M.J. Polydopamine and eumelanin: From structure-property relationships to a unified tailoring strategy. *Acc. Chem. Res.* **2014**, *47*, 3541–3550. [CrossRef] [PubMed]
11. Arzillo, M.; Mangiapia, G.; Pezzella, A.; Heenan, R.K.; Radulescu, A.; Paduano, L.; D'Ischia, M. Eumelanin buildup on the nanoscale: Aggregate growth/assembly and visible absorption development in biomimetic 5,6-dihydroxyindole polymerization. *Biomacromolecules* **2012**, *13*, 2379–2390. [CrossRef] [PubMed]
12. Drewnowska, J.M.; Zambrzycka, M.; Kalska-Szostko, B.; Fiedoruk, K.; Swiecicka, I. Melanin-like pigment synthesis by soil bacillus weihenstephanensis isolates from Northeastern Poland. *PLoS ONE* **2015**, *10*, e0125428. [CrossRef] [PubMed]

13. Harir, M.; Bellahcene, M.; Baratto, M.C.; Pollini, S.; Rossolini, G.M.; Trabalzini, L.; Fatarella, E.; Pogni, R. Isolation and characterization of a novel tyrosinase produced by Sahara soil actinobacteria and immobilization on nylon nanofiber membranes. *J. Biotechnol.* **2018**, *265*, 54–64. [CrossRef] [PubMed]
14. Le Roes-Hill, M.; Prins, A.; Meyers, P.R. *Streptomyces swartbergensis* sp. nov., a novel tyrosinase and antibiotic producing actinobacterium. *Antonie van Leeuwenhoek Int. J. Gen. Mol. Microbiol.* **2018**, *111*, 589–600. [CrossRef] [PubMed]
15. Claus, H.; Decker, H. Bacterial tyrosinases. *Syst. Appl. Microbiol.* **2006**, *29*, 3–14. [CrossRef] [PubMed]
16. Ito, S. IFPCS Presidential Lecture A Chemist's View of Melanogenesis. *Pigment Cell Res.* **2003**, *16*, 230–236. [CrossRef] [PubMed]
17. Plonka, P.M.; Grabacka, M. Melanin synthesis in microorganisms—Biotechnological and medical aspects. *Acta Biochim. Pol.* **2006**, *53*, 429–443.
18. Varga, M.; Berkesi, O.; Darula, Z.; May, N.V.; Palágyi, A. Structural characterization of allomelanin from black oat. *Phytochemistry* **2016**, *130*, 313–320. [CrossRef] [PubMed]
19. Almeida-Paes, R.; Frases, S.; de Sousa Araújo, G.; Evangelista de Oliveira, M.M.; Gerfen, G.J.; Nosanchuk, J.D.; Zancopé-Oliveira, R.M. Biosynthesis and functions of a melanoid pigment produced by species of the sporothrix complex in the presence of L-Tyrosine. *Appl. Environ. Microbiol.* **2012**, *78*, 8623–8630. [CrossRef] [PubMed]
20. Schmaler-Ripcke, J.; Sugareva, V.; Gebhardt, P.; Winkler, R.; Kniemeyer, O.; Heinekamp, T.; Brakhage, A.A. Production of pyomelanin, a second type of melanin, via the tyrosine degradation pathway in *Aspergillus fumigatus*. *Appl. Environ. Microbiol.* **2009**, *75*, 493–503. [CrossRef] [PubMed]
21. Ivins, B.E.; Holmes, R.K. Factors affecting phaeomelanin production by a melanin-producing (mel) mutant of Vibrio cholerae. *Infect. Immun.* **1981**, *34*, 895–899. [PubMed]
22. Li, C.; Ji, C.; Tang, B. Purification, characterization and biological activity of melanin from *Streptomyces* sp. *FEMS Microbiol. Lett.* **2018**, fny077. [CrossRef] [PubMed]
23. Ye, M.; Guo, G. yi; Lu, Y.; Song, S.; Wang, H. yan; Yang, L. Purification, structure and anti-radiation activity of melanin from Lachnum YM404. *Int. J. Biol. Macromol.* **2014**, *63*, 170–176. [CrossRef] [PubMed]
24. Sun, S.; Zhang, X.; Sun, S.; Zhang, L.; Shan, S.; Zhu, H. Production of natural melanin by *Auricularia auricula* and study on its molecular structure. *Food Chem.* **2016**, *190*, 801–807. [CrossRef] [PubMed]
25. Buszman, E.; Pilawa, B.; Zdybel, M.; Wilczyński, S.; Gondzik, A.; Witoszyńska, T.; Wilczok, T. EPR examination of Zn^{2+} and Cu^{2+} binding by pigmented soil fungi *Cladosporium cladosporioides*. *Sci. Total Environ.* **2006**, *363*, 195–205. [CrossRef] [PubMed]
26. Faccio, G.; Kruus, K.; Saloheimo, M.; Thöny-meyer, L. Bacterial tyrosinases and their applications. *Process Biochem.* **2012**, *47*, 1749–1760. [CrossRef]
27. Selinheimo, E.; Nieidhin, D.; Steffensen, C.; Nielsen, J.; Lomascolo, A.; Halaouli, S.; Record, E.; Beirne, D.O.; Buchert, J.; Kruus, K. Comparison of the characteristics of fungal and plant tyrosinases. *J. Biotechnol.* **2007**, *130*, 471–480. [CrossRef] [PubMed]
28. Plonka, P.M. Electron paramagnetic resonance as a unique tool for skin and hair research. *Exp. Dermatol.* **2009**, *18*, 472–484. [CrossRef] [PubMed]
29. Zdybel, M.; Pilawa, B.; Drewnowska, J.M.; Swiecicka, I. Comparative EPR studies of free radicals in melanin synthesized by *Bacillus weihenstephanensis* soil strains. *Chem. Phys. Lett.* **2017**, *679*, 185–192. [CrossRef]
30. Sealy, R.C.; Hyde, J.S.; Felix, C.C.; Menon, I.A.; Prota, G. Eumelanins and pheomelanins: characterization by electron spin resonance spectroscopy. *Science (80-)* **1982**, *217*, 545–547. [CrossRef]
31. Sealy, R.C.; Hyde, J.S.; Felix, C.C.; Menont, I.A.; Prota, G.; Swartz, H.M.; Persadt, S.; Habermant, H.F. Novel free radicals in synthetic and natural pheomelanins: Distinction between dopa melanins and cysteinyldopa melanins by ESR spectroscopy. *Proc. Natl. Acad. Sci. USA* **1982**, *79*, 2885–2889. [CrossRef] [PubMed]
32. Hannson, C.; Agrup, G.; Rorsman, H.; Rosengren, A.M.; Rosengren, E. Electron Spin Resonance Studies on Pheomelanins. *Acta Dermatovener* **1979**, *59*, 453–456.
33. Chikvaidze, E.N.; Partskhaladze, T.M.; Gogoladze, T.V. Electron spin resonance (ESR/EPR) of free radicals observed in human red hair: A new, simple empirical method of determination of pheomelanin/eumelanin ratio in hair. *Magn. Reson. Chem.* **2014**, *52*, 377–382. [CrossRef] [PubMed]
34. Selinheimo, E.; Gasparetti, C.; Mattinen, M.; Steffensen, C.L.; Buchert, J.; Kruus, K. Comparison of substrate specificity of tyrosinases from *Trichoderma reesei* and *Agaricus bisporus*. *Enzyme Microb. Technol.* **2009**, *44*, 1–10. [CrossRef]

35. Hernandez-Romero, D.; Sanchez-amat, A.; Solano, F. A tyrosinase with an abnormally high tyrosine hydroxylase/dopa oxidase ratio Role of the seventh histidine and accessibility to the active site. *FEBS J.* **2006**, *273*, 257–270. [CrossRef] [PubMed]
36. Commoner, B.; Townsend, J.; Pake, G.E. Free Radicals in biological materials. *Nature* **1954**, *4432*, 689–691. [CrossRef]
37. Pasenkiewicz-Gierula, M.; Sealy, R.C. Analysis of the ESR spectrum of synthetic dopa melanin. *Biochim. Biophys. Acta* **1986**, *884*, 510–516. [CrossRef]
38. Brogioni, B.; Biglino, D.; Sinicropi, A.; Reijerse, E.J.; Giardina, P.; Sannia, G.; Lubitz, W.; Basosi, R.; Pogni, R. Characterization of radical intermediates in laccase-mediator systems. A multifrequency EPR, ENDOR and DFT/PCM investigation. *Phys. Chem. Chem. Phys.* **2008**, *10*, 7284–7292. [CrossRef] [PubMed]
39. Pogni, R.; Baratto, M.C.; Sinicropi, A.; Basosi, R. Spectroscopic and computational characterization of laccases and their substrate radical intermediates. *Cell. Mol. Life Sci.* **2015**, *72*, 885–896. [CrossRef] [PubMed]
40. Napolitano, A.; De Lucia, M.; Panzella, L.; D'Ischia, M. The "benzothiazine" chromophore of pheomelanins: A reassessment. *Photochem. Photobiol.* **2008**, *84*, 593–599. [CrossRef] [PubMed]
41. Napolitano, A.; Di Donato, P.; Prota, G. New regulatory mechanisms in the biosynthesis of pheomelanins: Rearrangement vs. redox exchange reaction routes of a transient 2H-1,4-benzothiazine-o-quinonimine intermediate. *Biochim. Biophys. Acta–Gen. Subj.* **2000**, *1475*, 47–54. [CrossRef]
42. Stoll, S.; Schweiger, A. EasySpin, a comprehensive software package for spectral simulation and analysis in EPR. *J. Magn. Reson.* **2006**, *178*, 42–55. [CrossRef] [PubMed]

Sample Availability: Samples of the Sc-Ms1 natural melanin and enzymic synthesized melanins are available from the authors.

THE JOURNAL OF PHYSICAL CHEMISTRY B

pubs.acs.org/JPCB Article

Paramagnetism and Relaxation Dynamics in Melanin Biomaterials

Maher Al Khatib, Jessica Costa, Maria Camilla Baratto, Riccardo Basosi, and Rebecca Pogni*

Cite This: J. Phys. Chem. B 2020, 124, 2110−2115 Read Online

ACCESS | Metrics & More | Article Recommendations | Supporting Information

ABSTRACT: Spectroscopical characterization of melanins is a prior requirement for the efficient tailoring of their radical scavenging, ultraviolet−visible radiation absorption, metal chelation, and natural pigment properties. Electron paramagnetic resonance (EPR), exploiting the common persistent paramagnetism of melanins, represents the elective standard for the structural and dynamical characterization of their constituting radical species. Although melanins are mainly investigated using X-band (9.5 GHz) continuous wave (CW)-EPR, an integration with the application of Q-band (34 GHz) in CW and pulse EPR for the discrimination of melanin pigments of different compositions is presented here. The longitudinal relaxation times measured highlight faster relaxation rates for cysteinyldopa melanin, compared to those of the most common dopa melanin pigment, suggesting pulse EPR spin−lattice relaxation time measurements as a complementary tool for characterization of pigments of interest for biomimetic materials engineering.

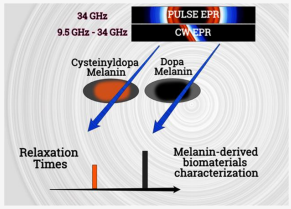

INTRODUCTION

Bioinspired materials are designed to mimic the biological, chemical, and physical properties of extraordinary materials present in nature. The variety with which nature expresses itself can be exploited for the realization of biocompatible materials to support the needs and challenges of a green-economy logic. In this context, melanin pigments have attracted an increasing degree of attention because of their potential applications in the realization of optoelectronical and biomedical devices.[1−11] Melanins are ubiquitous pigments present in nature, which exhibit peculiar adhesive properties and a wide ultraviolet−visible (UV−vis) light absorption spectrum and are capable of acting as mixed ionic-electronic conductors, marked metal ions chelator and of free radical scavenging activities.[12−24]

Because of the lower immunoresponse in in vitro tests, melanins have been proposed for electromedical device coatings.[8] Furthermore, melanins are commonly known for their characteristic black-to-reddish color span, and the exploitation of their structural and geometrical spatial organization has been proven successful for the realization of structural colors.[25−32] In fact, melanin's highly heterogeneous structural and geometrical features on the nano- and microscale contribute to most of their characteristic physicochemical properties, such as the increasing absorption trend toward the blue region of the UV−vis spectrum.[33] This high structural heterogeneity poses a challenge for melanin characterization, which is necessary for the controlled design and engineering of functional melanin materials.[34,35] With the state of the art technology, the most successful characterization of melanin pigments is being achieved using continuous wave (CW) electron paramagnetic resonance (EPR) spectroscopy, which exploits the characteristic persistence of free radical species common to all melanins to extract structural and dynamical information (e.g., free radical composition).[36−42] EPR investigation, together with the support of computational studies, helped to identify 5,6-dihydroxyindole (DHI) and 5,6-dihydroxyindole-2-carboxylic acid (DHICA) as the main constituents of the most common melanin form found in nature, eumelanin (also known as dopa melanin), whereas cysteinyldopa-derived units have been found as characteristic components of pheomelanin (also known as cysteinyldopa melanin).[5,13,43−46] Electrochemical fingerprinting has been used to suggest that natural eumelanin pigments contain porphyrin-like proto-molecules composed of DHI/DHICA tetramers, whereas recent computational investigations describe melanins as a mixture of low-molecular-weight oligomers.[43,47]

In this paper, the paramagnetic properties of enzymatically produced dopa melanin and cysteinyldopa melanin have been probed by the use of Q-band (34 GHz) pulse EPR and Q- and X-band (9 GHz) CW multifrequency EPR. The use of selective microwave pulses at Q-band frequencies was employed to measure the longitudinal relaxation times of these two different melanin pigments, providing the evidence that faster relaxation dynamics are present in cysteinyldopa melanin and that the EPR pulse technique can represent a useful and complementary tool to discriminate between the two different pigments.

Received: December 20, 2019
Revised: February 21, 2020
Published: February 27, 2020

https://dx.doi.org/10.1021/acs.jpcb.9b11785
J. Phys. Chem. B 2020, 124, 2110−2115

EXPERIMENTAL SECTION

Sample Preparation. Two different samples were prepared by the oxidative activity of *Trametes versicolor* laccase (12.9 U mg^{-1}) in 100 mM phosphate buffer (pH = 7.1) and dopa (6.57 mg/mL) (1:1000 Lac/dopa molar ratio) for dopa melanin synthesis and in 1:2 dopa/cysteine molar ratio in 100 mM acetate buffer (pH = 4.5) for cysteinyldopa synthesis.[13] The formation of markedly insoluble black and reddish pigments was observed. The synthesis was performed at room temperature in air under stirring for 16 h. The samples were dried under nitrogen flux and collected as dry powders. The powders were inserted within cylindrical suprasil capillaries for EPR Q-band measurements (WG-222T-RB, Cortecnet Europe, France) with ID × OD equal to 1.1 × 1.6 mm (where ID and OD represent the inner and outer diameters of the cylinder, respectively). The same samples were used for CW X- and Q-band and pulse Q-band EPR measurements. Possible sample hydration cannot be ruled out.

EPR Experimental Setup. EPR spectra were measured with a Bruker ELEXSYS E580 Super Q-FT spectrometer, equipped with an ER 5107D2 probehead, a CF935 continuous-flow helium cryostat (Oxford Instruments), and an ITC 502 temperature controller (Oxford Instruments) for CW and pulse Q-band EPR measurements. The CW X-band spectra and spin quantitation measurements were performed using a Bruker ER 049X microwave bridge with 4122SHQE/0208 cavity. The spin quantitation was carried out against an internal reference (Bruker) of irradiated solid alanine (3 mm length, 5 mm diameter) sealed under a N_2 atmosphere and containing a total of $2.05 \times 10^{-7} \pm 10\%$ spins, using the SpinCounting program provided in the Xepr software (Bruker).

Q-Band Pulse Experiments. The echo detected field sweep (EDFS) spectra of the two melanin samples were acquired with a $\pi/2$-τ-π echo sequence ($\pi/2$ = 42 ns and π = 84 ns). A picket fence saturation recovery (PFSR) sequence (Scheme 1) was used for the measurement of longitudinal relaxation times.

Scheme 1. PFSR Sequence[a]

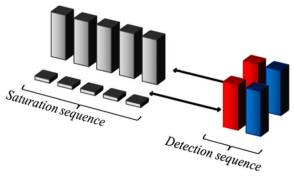

[a]Saturation and detection microwave pulses were used to measure the longitudinal relaxation times.

The region of the EPR spectra corresponding to the maximum of absorption was irradiated with a train of 29 saturating rectangular $\pi/2$ microwave pulses (higher gray pulses in Scheme 1), and the value of the residual magnetization was sampled with rectangular pulses of $\pi/2$-τ-π echo detection sequence (red and blue pulses, respectively). In order to assess the effective saturation recovery, the equilibrium value of the magnetization was acquired by running a PFSR experiment where the saturating pulses were turned off (lower gray pulses).

RESULTS AND DISCUSSION

The CW-EPR technique is widely employed for the characterization of melanin-free radical species. However, the *g*-value, intensity, and line shape of the spectrum are the sole observables obtained from a CW-EPR spectrum as no hyperfine structure is observed. In the context of relaxation time measurements, melanin pigment characterization was carried out in the pioneering work by Sarna and Hyde on 1978, whereas pulse EPR has been long underexploited for melanin radical characterization, with the exception of the landmark X-band pulse EPR paper of Okazaki et al. dating back to 1985.[48,49]

In Figure 1a,b, the EPR spectra recorded at increasing microwave power (maximum power value, M_0 = 144.5 mW) for the dopa melanin (g_{iso} = 2.0036 ± 0.0002, Figure 1a) and cysteinyldopa melanin (g_{iso} = 2.0050 ± 0.0002, Figure 1b) samples are shown. The dopa melanin free radical signal (peak to peak signal amplitude, ΔB_{pp} = 0.5 ± 0.1 mT at a microwave power of M = 1.46 mW) is commonly interpreted as originating from the concomitant presence of carbon-centered ($g \approx 2.0032$) and semiquinone ($g \approx 2.0045$) free radical species, whose respective contributions to the EPR signals are a function of the hydration level and pH of the sample.[50] The free radical signal recorded in cysteinyldopa melanins, on the other hand, with its higher *g* value ($g \approx 2.0050$) and broader line shape (central line peak-to-peak signal amplitude, ΔB_{pp} = 3.2 ± 0.1 mT, at a microwave power of M = 1.46 mW), is attributed to the presence of semiquinonimine free radical species.[51,52]

The intensity increase of the X-band EPR signal for dopa and cysteinyldopa samples reaches a maximum and then decreases with higher microwave power levels (Figure S1). The same trend is also evident in the EPR spectra recorded at Q-band (Figure S2). This progress of the EPR lines suggests a homogeneous line broadening with the absence of the so-called spin-islands with a free radical spin density equal to ~5.84×10^{13} spins/mm^3 for dopa melanin and ~2.20×10^{13} spins/mm^3 for cysteinyldopa melanin.[41]

To investigate the possible use of relaxation time as a novel observable to differentiate melanin samples, pulse Q-band EPR (34 GHz) was employed for longitudinal relaxation time (T_1) determination. The solid-state Q-band EPR experiments will be of great help as at this frequency, the *g* values and anisotropies of the different radical species are better solved. Room-temperature Q-band EDFS spectra of the samples were first recorded in order to set the region of spectra to be selected for further investigations (black lines in Figure 1c,d). Rectangular microwave pulses of $\pi/2$ = 42 ns and π = 84 ns (full-width-half-height linewidth of ~29 and 14 MHz, respectively, red and blue lines in Figure 1c,d) were then optimized for the relaxation study sequences further used. The spectral coverage of the $\pi/2$ and π microwave pulses was centered in correspondence to the maximum of the absorption spectra of the dopa melanin and cysteinyldopa melanin. The room-temperature phase memory time (T_M) of the two pigments was measured in place of the transverse relaxation time T_2 in order to take into account the effect of instantaneous diffusion. The latter can contribute to the transverse relaxation process at the relatively low concentrations of paramagnetic centers in the samples (lower than 10^{15} spins/mm^3).[53] The phase memory time T_M was extracted from the echo decay curves (Figure S3) using a mono-

https://dx.doi.org/10.1021/acs.jpcb.9b11785
J. Phys. Chem. B 2020, 124, 2110−2115